Available online at www.sciencedirect.com
SCIENCE DIRECT®
Journal of Chromatography A, 1092 (2005) 142–148
JOURNAL OF CHROMATOGRAPHY A
www.elsevier.com/locate/chroma

Analysis of applying different solvents for the mobile phase and for sample injection

Knut Gedicke [a], Magdalena Tomusiak [b], Dorota Antos [b,*], Andreas Seidel-Morgenstern [a,c]

[a] *Chair of Chemical Process Engineering, Otto-von-Guericke-University, 39106 Magdeburg, Germany*
[b] *Department of Chemical and Process Engineering, Rzeszów University of Technology, 35-959 Rzeszów, Al. Powstancow Warszawy 6, Poland*
[c] *Max-Planck-Institute for Dynamics of Complex Technical Systems, 39106 Magdeburg, Germany*

Available online 3 March 2005

Abstract

Overloading a chromatographic column with a compound possessing low solubility in the mobile phase has been investigated. In order to increase the concentration of injection a strong solvent for dissolving the feed was used. The injection of such concentrated samples brings the risk of triggering undesired crystallisation processes. A model system has been investigated with ethanol–water as the mobile phase and DL-threonine as the sample dissolved in pure water. Under extreme overloaded conditions band splitting was observed. Measurements of the adsorption isotherms and systematic solubility studies were carried out. For the process analysis a simplified mathematical model was applied. The simulations of the band profiles were compared with the experimental data.

Keywords: Preparative chromatography; Caolumn overloading; Band splitting; Solubility limits; Crystallisation

1. Introduction

In the last years chromatographic methods have been increasingly applied for the preparative separation of isomers, enantiomers, oligosaccharides and proteins. This is due to the improved availability of selective stationary phases [1], the improved understanding of front migration phenomena in fixed beds under overloaded (nonlinear) conditions [2,3] and the development of more sophisticated multicolumn processes allowing continuous operation in an industrial scale [4]. The application of chromatography in a large scale requires optimisation of operating conditions, which should assure minimal cost of the separation. Columns are usually overloaded in preparative elution chromatography to achieve that goal. It is well known that concentration overloading is superior to volume overloading [2]. Hereby a typical restriction is given by limited solubility of the samples in the mobile phase selected to achieve good separations. A possibility to increase the column load is to use for the injection a solvent in which the sample has a higher solubility. The elution strength of such solvents is usually larger than that of the mobile phases. The use of an extra-solvent to dissolve the feed components is common in industrial practice for systems with low solubility of the samples in the mobile phase [5]. Jandera and Guiochon [6] reported deformation and splitting of elution profiles at the column outlet for the example of non-aqueous reversed-phase chromatography. Feng et al. [7] observed similar phenomena for hydrophobic interaction chromatography of proteins. An additional obstacle is that the injection of very concentrated samples brings the risk of triggering undesired crystallisation effects, which may reduce the permeability of the chromatographic system due to blocking phenomena.

The aim of this work was to bring further insight in the application of a stronger solvent for injection than that for the elution. The research has been performed in the following stages: (a) solubility measurements of the selected substance, which exhibits low solubility in the solvents typically used as a mobile phase, (b) chromatographic experiments under strongly overloaded conditions, (c) analysing the influence of the mobile phase composition on the adsorption equilib-

* Corresponding author. Tel.: +48 17 865 17 30; fax: +48 17 854 36 55.
E-mail address: dorota_antos@prz.rzeszow.pl (D. Antos).

0021-9673/$ – see front matter © 2005 Elsevier B.V. All rights reserved.
doi:10.1016/j.chroma.2005.02.059

rium of the component studied, (d) developing and validating a simplified mathematical model. Another goal of this work was to check if there exist such extreme conditions, where precipitation within the chromatographic system occurs. In order to study systematically the overloading effect a chromatographic system was chosen, which consisted of just one solute with reasonable retention in the mobile phase.

2. Experimental procedures and chemicals

A summary of the chromatographic system chosen for the investigation is given in Table 1. Ethanol was of HPLC grade (Merck, Darmstadt, Germany). Deionised water was used and further purified using a Milli-Q-Gradient system (Millipore, Billerica, MA, U.S.A.). DL-Threonine (>99%) was obtained from Merck (Darmstadt, Germany). Lichroprep NH_2 25–40 μm (Merck, Darmstadt, Germany) was used as the stationary phase capable to retain threonine. The column was packed in our laboratory, by subsequent filling and compression (due to slight thumping on the column) of dry stationary phase.

The solubility of DL-threonine in solvents of different water contents was measured in our laboratory. In a series of experiments, a surplus of DL-threonine was equilibrated with solvent at 20 °C for 24 h. The temperature of the stirred suspension was controlled (±0.1 K) with a Polystat CC3 thermostat (Peter Huber Kältemaschinenbau, Offenburg, Germany). A sample of 10–20 ml of the liquid was taken after equilibration. The liquid was completely evaporated and the threonine content was determined gravimetrically [8]. The mass of the sample before and after evaporation was measured (±0.1 mg) with a microbalance AT261 by Mettler Toledo (Giessen, Germany).

For the elution experiments a conventional HPLC system was used, consisting of a Waters 600E quaternary low-pressure gradient pump (Waters, Milford, MA, U.S.A.) and a UV-detector (Knauer, Berlin, Germany). The detection was done at 215 nm. The temperature of the column and the manual injection valve (integrated in the thermostat) was controlled at 20 °C (Jetstream II, Knauer, Berlin, Germany). Only full loop injections were performed with sample loops of 10, 100, 1000 and 2000 μl. Each experiment was repeated at least twice.

Frontal analysis experiments of consecutive breakthroughs (20 steps) were carried out at 9 different volume fractions of water in the mobile phase (i.e., 0.2–1). The maximum concentrations of these experiments were close to the solubility limit of threonine in the mobile phase. These experiments have been performed using the low-pressure gradient of the pump and were used also to calibrate the detector at different water contents. The flow rate of all experiments was 1.97 ml/min and has been permanently verified with a flowmeter (Phase Separations, Deeside, U.K.).

Table 1
Summary of the experimental system

Solute	DL-Threonine
Mobile phase	Water–ethanol of various compositions
Feed solvent	Water
Stationary phase and column	LiChroprep NH_2, 24–40 μm, 0.46 cm × 25 cm, $\varepsilon = 0.792$

3. Results

3.1. Solubility of DL-threonine in the mobile phases and in the injection media

Fig. 1 shows the solubility of DL-threonine at 20 °C for different water contents in the solution. The applied constant injection concentration is also depicted. The solubility was approximated with an empirical function fitted to the experimental data using a nonlinear curve fit (correlation coefficient $r^2 = 0.998$, see Table 2 for details).

$$C_{S,DL} = 0.77 \exp(6.01 y_{H_2O}) \quad (1)$$

$C_{S,DL}$ and y_{H_2O} are the saturation concentration of DL-threonine in g/l and the volume fraction of water in the solution, respectively.

3.2. Elution profiles

The mobile phase compositions of the overloaded elution experiments were $y_{H_2O} = 0.1$, 0.2, 0.3 and 0.4 volume

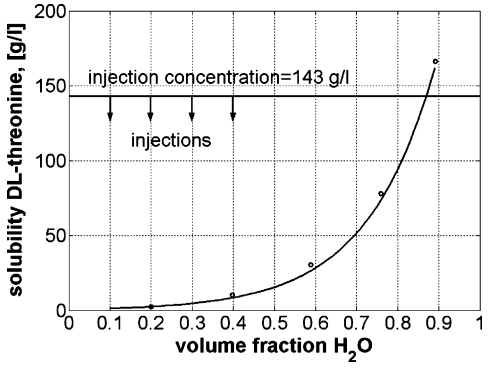

Fig. 1. Solubility of DL-threonine at 20 °C in ethanol–water mixtures. Symbols: experimental data points, line: empirical function (Eq. (1)). The arrows indicate the water content of the mobile phases at which elution experiments were performed, while the horizontal line depicts the injection concentration.

Table 2
Solubility of DL-threonine in ethanol/water mixtures at 20 °C

H_2O:EtOH$_{v/v}$	y_{H_2O}	$C^{exp}_{S,DL}$	$C_{S,DL}$ calc. with Eq. (1)
20:80	0.20	2.4	2.6
40:60	0.40	10.3	8.5
60:40	0.59	29.3	26.7
80:20	0.76	78.2	74.2
100:0	0.89	165.7	162.0

fraction of water and the corresponding solubility (Eq. (1)) in the mobile phase was $C_{S,DL}$ = 1.4, 2.6, 4.6 and 8.5 g/l, respectively. The injection solvent was water and the injection concentration was 143 g/l for all experiments. Note that the injection concentration was much higher than the solubility of DL-threonine in the mobile phase. However, precipitation or at least crystallisation of threonine large enough to reduce the permeability of the column (thus increasing the pressure drop) was not observed during these experiments. This was surprising, since injections were performed up to 60% of column fluid volume (3.29 ml). Due to the large surface area provided by the stationary phase, crystallisation can be expected to occur instantaneously once a supersaturation is present with the system. Nevertheless, our results are in agreement with the observations reported earlier by Szanya et al. [9] for the separation of two steroids, where the displacement of the less adsorbed component by stronger adsorbed component caused precipitation of the former one within the column. However, for this system column blocking has not been reported either.

Fig. 2 shows the evolution of the elution profiles of threonine with increased injection volume. At the chosen wavelength the signal of threonine was independent of the water content in the mobile phase. Blank injections of water (without threonine) resulted in negligible detector responses. The retention of the sample increased with decreased amount of the strong solvent water (evident especially for 100 μl injections, Fig. 2a–d, left plot). The sample elutes as a single peak for 100 μl injections. For larger injection volumes a part of the sample travels faster with the injection media water resulting in a peak splitting, which becomes more pronounced for decreased water contents in the mobile phase (see Fig. 2a–d, middle and right plots). Note that the enantiomers of DL-threonine are not separated in this achiral chromatographic system. In this environment the enantiomers behave as a single component.

This band splitting phenomenon is in agreement with the results reported by Jandera and Guiochon [6] for non-aqueous reversed-phase chromatography and by Feng et al. [7] for hydrophobic interaction chromatography of proteins.

3.3. Determination of adsorption isotherm

To gain further insight in this phenomenon we determined the adsorption isotherms of the sample at nine different water contents in the mobile phase. The mobile phase component water was found to deactivate progressively the adsorbent and to reduce the adsorption capacity of the polar adsorbent (although the manufacturer recommends water as a mobile phase for this stationary phase). Nevertheless, for the purpose of our study this system was found to be a good example for studying the crystallisation phenomenon because of high solubility of the sample in water and reasonable time of its retention in the mobile phase containing ethanol–water.

Frontal analysis required a number of experiments involving equilibration of the adsorbent with the water-rich mobile phases and could, due to the mentioned deactivation, not be successfully used to determine the adsorption equilibria on the stationary phase precisely. Nevertheless, frontal analysis of consecutive breakthroughs was applied to get information of the shape of the isotherms at different water contents in the mobile phase.

The bi-Langmuir model has been used to correlate the concentration of the sample in the mobile and the solid phase. The model assumes adsorption mechanism on the heterogeneous surface containing two energetically different adsorption sites: site “1” with high adsorption energy accounted for by high equilibrium constant and site “2” with a low adsorption energy and a low equilibrium constant:

$$q^*_{DL} = \frac{a_1(y_{H_2O})C_{DL}}{1 + b_1(y_{H_2O})C_{DL}} + \frac{a_2(y_{H_2O})C_{DL}}{1 + b_2(y_{H_2O})C_{DL}} \quad (2a)$$

where C_{DL} is the concentration of the sample in the mobile phase, q^*_{DL} the concentration in the solid phase at equilibrium with C_{DL}, y_{H_2O} the volume fraction of water, a corresponds to retention of the sample on site 1 or 2 and b corresponds to the equilibrium constant for site 1 or 2.

If the value of the equilibrium constant for the site “2” is very low the bi-Langmuir equation can be simplified to the three parameter form, which was used in this work:

$$q^*_{DL} = \frac{a_1(y_{H_2O})C_{DL}}{1 + b(y_{H_2O})C_{DL}} + a_2(y_{H_2O})C_{DL} \quad (2b)$$

For a multi-component mobile phase (here ethanol–water) the isotherm coefficients can be considered as apparent factors lumping the contributions of all constituents of the mobile phase to the adsorption equilibrium. These coefficients are functions of the mobile phase composition, in our case expressed as a function of the water content y_{H_2O}.

After accomplishing the frontal analysis the retention time of small pulses of the sample were measured again for various mobile phase compositions. Due to the adsorbent deactivation mentioned above, some differences in retention have been found for the pulses recorded before and after frontal analysis. Therefore, finally for evaluation of the isotherm coefficients a peak fitting method (e.g., James et al. [10]) of the chromatograms registered before the experiments of frontal analysis was employed.

For peak fitting overloaded chromatograms registered at different water contents were selected, for which solvent and sample were well separated at the column outlet, i.e., interactions between sample and solvent could be neglected. The overloaded band profiles exhibited strong peak tailing (see e.g., Figs. 2 and 4) characteristic for heterogeneous adsorption mechanism. Such a peak shape was not reproduced correctly by the use of the Langmuir model, while the three parameters bi-Lagmuir model (Eq. (2b)) was found to be sufficiently accurate.

The isotherm coefficients of Eq. (2) were determined by the use of a standard optimisation tool; i.e., Marquardt–Levenberg optimisation routine, for each volume fraction of water in the mobile phase. The following empiri-

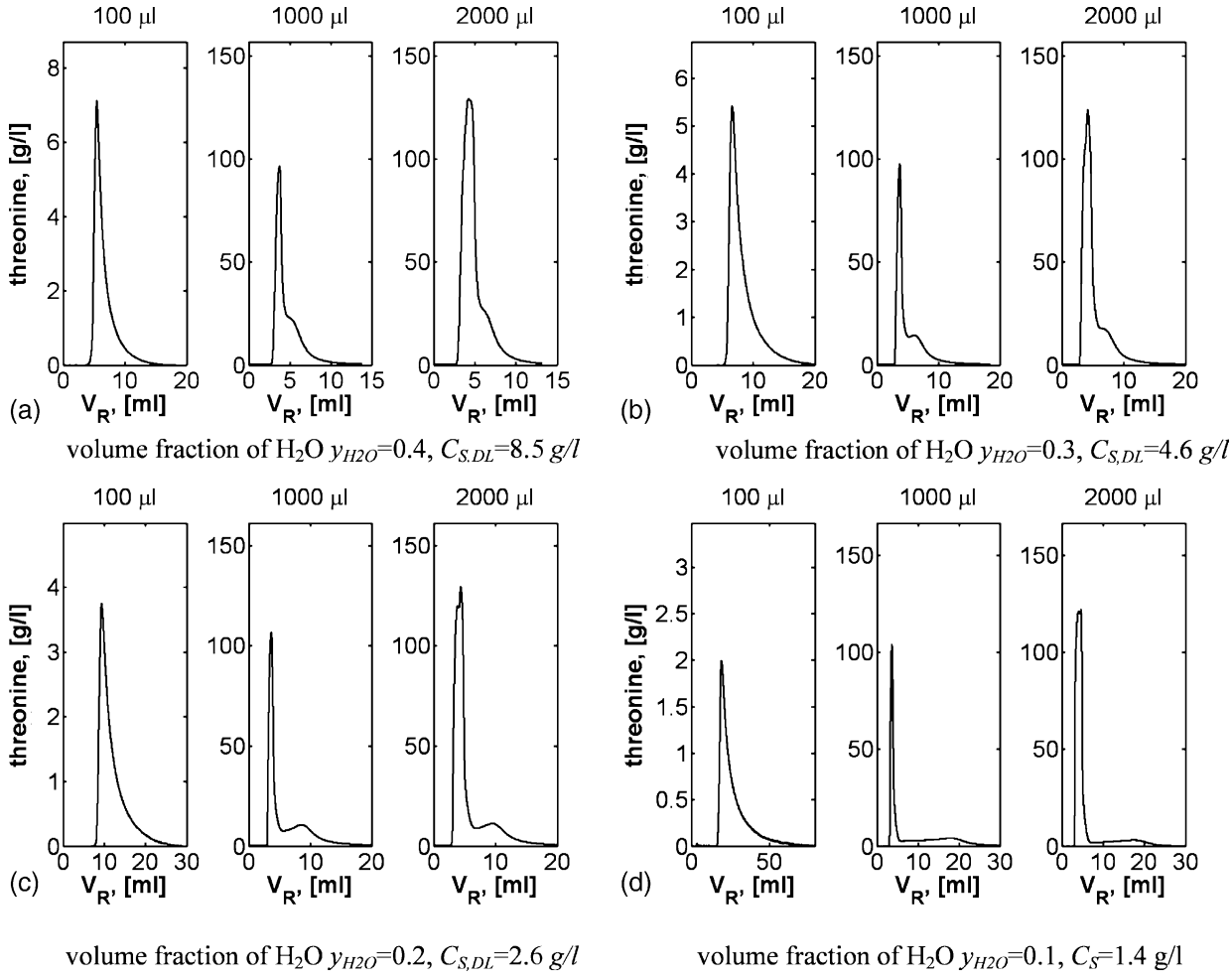

Fig. 2. Evolution of experimental elution profiles of threonine with increasing injection volume (C_{inj} = 143 g/l) and for decreasing water contents in the mobile phase (a–d). $C_{S,DL}$ denotes the saturation concentration of DL-threonine in the applied mobile phase and was calculated with Eq. (1).

cal functions were fitted to the obtained isotherm parameters of threonine.

$$a_1 = p_{a_1} y_{H_2O}^{-ma_1} + r_{a_1}; \quad a_2 = p_{a_2} y_{H_2O}^{-ma_2} + r_{a_2};$$
$$b = p_b y_{H_2O}^{-mb} + r_b \tag{3}$$

The coefficients of these functions are shown in Table 3 and the resulting isotherms are depicted in Fig. 3.

The loading of water could be neglected since pulse experiments at different water contents in the mobile phases investigated (i.e., 0.2–0.9) showed no retention.

Table 3
Coefficients of Eq. (3) correlating the isotherm parameters of threonine (Eq. (2b)) with the water content in the solution

Isotherm parameter (Eq. (2))	p	m	r
a_1	0.307	2.077	6.016
b (l/g)	0.002	2.954	0.614
a_2	0.5	1.485	0

3.4. Column model

The well-known equilibrium dispersive model [3] has been used to simulate the elution profiles of the sample as

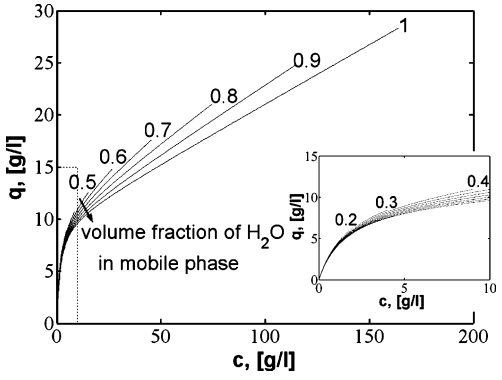

Fig. 3. Isotherms of threonine at 20 °C as calculated (Eqs. (2b) and (3)) from peak fitting method. Parameters as listed in Table 3. Isotherms are extrapolated up to the solubility limit in the mobile phase.

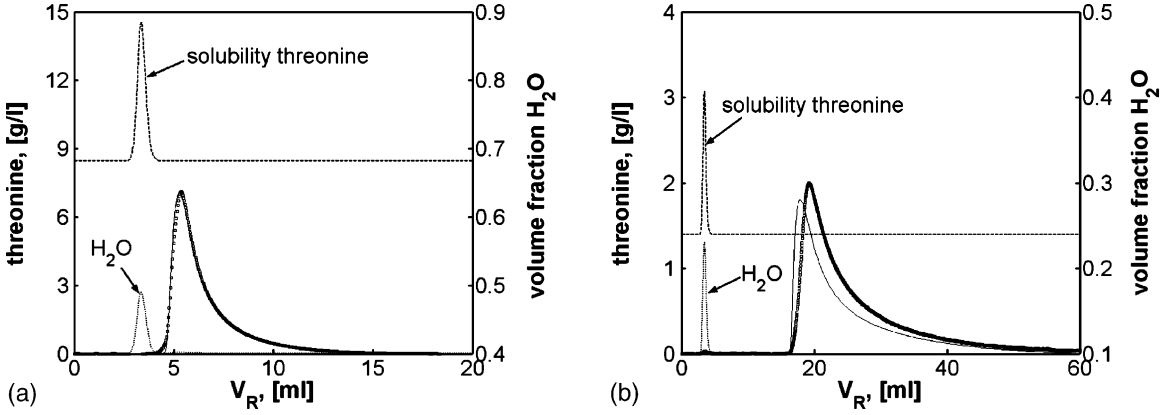

Fig. 4. Experimental (symbols) and simulated (solid line) elution profile of threonine at the column outlet for 100 μl injections. Solubility of threonine (dashed line) calculated with Eq. (1) corresponding to the simulated elution profile of water (dotted line, right axis): (a) at $y_{H_2O} = 0.4$ vol.-fr. in the mobile phase, (b) at $y_{H_2O} = 0.1$ vol.-fr. in the mobile phase.

well as of the solvent water.

$$\varepsilon\frac{\partial C_i}{\partial t} + (1-\varepsilon)\frac{\partial q_i}{\partial t} + u\frac{\partial C_i}{\partial z} = D_{\text{app},i}\frac{\partial^2 C_i}{\partial z^2}$$

$$\text{with} \quad D_{\text{app},i} = \frac{uL}{2N_i} \tag{4}$$

where $D_{\text{app},i}$ is an apparent dispersion coefficient. u, L, N_i, t, z and ε are fluid velocity, column length, number of theoretical plates of component i, time, space coordinate and the overall porosity of the column, respectively. The number of theoretical plates has been determined experimentally and was 250 for water and 90 for threonine. This model coupled with adequate initial and boundary conditions was discretized by the use of the method of orthogonal collocation on fixed elements and solved with the VODE procedure (procedure available in http://www.netlib.org), which automatically chooses the time increment in order to guarantee the required accuracy of the solution. The number of collocations points was high enough to assure numerical convergence of the solution. Details of the discretization method of orthogonal collocation used in this work can be found elsewhere [11,12].

4. Discussion

The band profiles of threonine as well as the injection solvent water were calculated (numerical solution of Eqs. (2)–(4)) and are depicted for selected examples in Figs. 4 and 5. Directly after injection the front part of threonine travels with a velocity corresponding to the retention behaviour of threonine in water. If the sample volume is large enough, that non-retained water and threonine do not separate, then some amount of threonine elutes together with water (see Fig. 5). The rear part of the sample separates from the injection solvent (as it is the case for small injection volumes, Fig. 4) and travels then with a lower velocity corresponding to the adsorption isotherm valid for the mobile phase composition. These different travelling velocities cause the observed band splitting (see Figs. 2 and 5).

The agreement between the calculated and the experimental elution profiles is quite satisfactory, considering that the isotherm parameters reflect just a ‘snapshot’ of the mentioned transient adsorption behaviour (due to the aforementioned temporal degradation of the stationary phase). The agree-

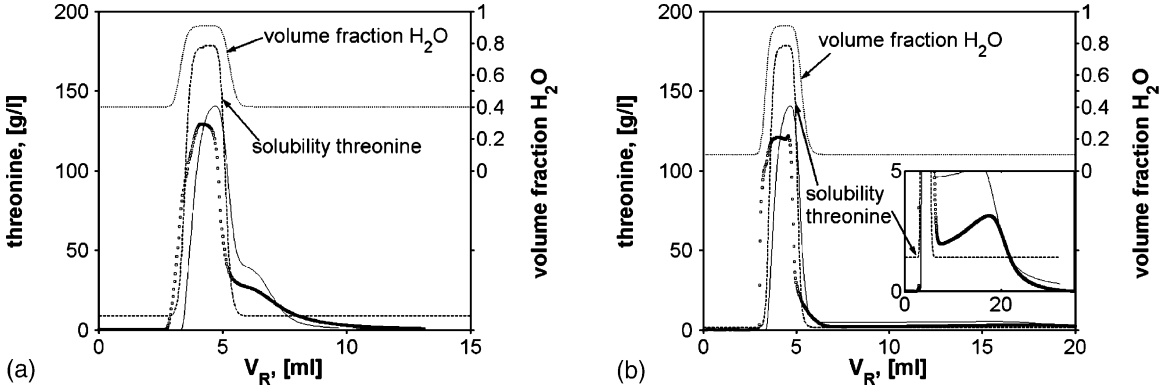

Fig. 5. Experimental (symbols) and simulated (solid line) elution profile of threonine at the column outlet for 2000 μl injections. Solubility of threonine (dashed line) calculated with Eq. (1) corresponding to the simulated elution profile of water (dotted line, right axis): (a) at $y_{H_2O} = 0.4$ vol.-fr. of water in the mobile phase, (b) at $y_{H_2O} = 0.1$ vol.-fr. of water in the mobile phase.

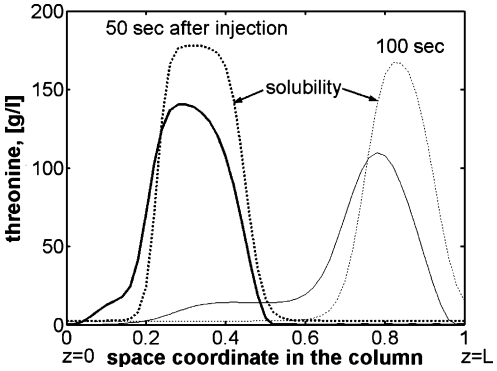

Fig. 6. Simulated concentration (solid lines) and solubility (dotted lines) distribution of threonine in the column 50 s (thick lines) and 100 s (thin lines) after injection ($y_{H_2O} = 0.2$ and $V_{inj} = 1000\,\mu l$).

ment for 100 μl injections (Fig. 4) is better than the agreement for the larger injection volumes (Fig. 5), because the 100 μl injections were taken also for the peak fitting method. The applied mathematical strategy, already used for prediction of gradient elution [13,14] is capable to account for the band splitting observed for large injection volumes. In our model precipitation was not taken into account, contrary to Jandera and Guiochon [6], who used a similar model. These authors reported qualitative agreement of the model predictions with their experimentally determined elution profiles, once the model also accounted for precipitation (for details see [6]). This was not necessary in our case, where already the band profiles calculated with the fitted isotherm data and without a limitation of a maximal fluid phase concentration showed qualitative similar behaviour like the experimental elution profiles.

Figs. 4 and 5 show, besides a comparison of the experimental and the simulated elution profiles of threonine, also the water content simulated at the column outlet and the corresponding solubility of threonine (calculated with Eq. (1)). The solubility limit is not exceeded at the column outlet only for the 100 μl injection with a mobile phase composition $y_{H_2O} = 0.4$ (Fig. 4a). The concentrations of threonine exceed to a large extent the solubility of threonine for all other experiments (Figs. 4b and 5).

Fig. 6 depicts an example of concentration profiles calculated within the column and the local solubility (related to the local water concentration) for two different times after injection. The development of the band splitting is clearly visible, as well as the spreading of the sample over almost the entire length of the column. Concentrations of threonine above the local solubility limit indicate the danger of precipitation in the column (Fig. 6) and at the column outlet (Figs. 4b and 5a, b). Even though we observed no blocking of the column, threonine precipitated during one experiment ($y_{H_2O} = 0.1$, $V_{inj} = 2000\,\mu l$) in the tubing after the detector (which actually caused a damage of the detector cell). A reason could be, that even if crystals form in the column due to local supersaturation (as it seemed to be the case in [6,9]), these could be too small to result in local reduction of permeability of the column. On the other hand, the cross sectional area of the tubing is much smaller than that of the column. Precipitation in the tubing will therefore more likely result in blocking of the flow path.

In order to predict crystallisation phenomena properly, one needs to determine in detail kinetics of nucleation, growth and dissolution in presence of the heterogeneous surface provided by the stationary phase. Macro-kinetic isothermal growth/dissolution experiments in the presence of stationary phase may be possible, but the determination of heterogeneous nucleation rates remains a challenging future task, since the nuclei will contain just a few molecules [15]. Although different theories exist to predict heterogeneous nucleation rates [15–17], the authors did not feel confident enough to apply these methods here without experimental proofs.

The 1000 and 2000 μl injections represent rather unrealistic sample volumes for such a small column. Note, that by applying water as a feed solvent rather than the mobile phase, the amount injected was increased by factors of about 17, 31, 57 and 95 compared to the amount applicable in the mobile phase (using the same injection volume). This states the potential of applying a different solvent for the injection. Of course some other aspects have to be accounted for. The injection solvent must separate quickly from the sample, such that band splitting is suppressed and the better separation properties of the mobile phase can be exploited. For safety reasons the concentration of band profiles at the column outlet should exceed the solubility limits only slightly.

5. Summary

The evolution of significantly overloaded elution profiles of threonine, injected in water on an NH_2-column at a much higher concentration than the solubility limit in the mobile phase, has been illustrated for mobile phase compositions containing 0.1–0.4 vol.-fr. of water. Significant band splitting was observed for large sample amounts. A simplified mathematical model as it is often used to predict gradient elution was applied. Measurements of the adsorption equilibria and solubility measurements for mobile phases containing varying concentration of the feed solvent have been performed. The resulting adsorption data have been used to correlate the isotherm coefficients of the sample with the local concentration of the strong solvent within the column. The solubility measurements have been exploited for calculation of the local solubility limits related to the local mobile phase composition. These relationships have been included as model parameters into the model of the column dynamics, which allowed calculating concentration profiles for the sample as well as for the strong solvent water. The model qualitatively reproduced the change of peak shapes as an effect of the differences in the adsorption of the sample in the feed solvent and in the solution.

Acknowledgements

The authors wish to express their gratitude to Dragomuir Sapoundjiev, who performed the laborious solubility measurements. This work was supported in part by the COMODEC Centre of Excellence project, co-funded by the European Community (#8216) and the German Academic Exchange Service (DAAD).

References

[1] Section 'Columns', J. Chromatogr. A 658 (2002) 67–205.
[2] G. Guiochon, S. Golshan-Shirazi, A.M. Katti, Fundamentals of Preparative and Nonlinear Chromatography, Academic Press, Boston, 1994.
[3] G. Guiochon, J. Chromatogr. A 965 (2002) 129.
[4] D.M. Ruthven, C.B. Ching, Chem. Eng. Sci. 44 (1989) 1011.
[5] G. Mann, Schering AG, Berlin, Germany, personal communication.
[6] P. Jandera, G. Guiochon, J. Chromatogr. 588 (1991) 1.
[7] W. Feng, X. Zhu, L. Zhang, X. Geng, J. Chromatogr. A 729 (1996) 43.
[8] D. Sapoundjiev, Ph.D. thesis, Otto-von-Guericke-University, Germany, in preparation.
[9] T. Szanya, J. Argyelan, S. Kovats, L. Hanak, J. Chromatogr. A 908 (2001) 265.
[10] F. James, M. Sepúlveda, F. Charton, I. Quinones, G. Guiochon, Chem. Eng. Sci. 54 (1999) 1677.
[11] K. Kaczmarski, M. Mazzotti, G. Storti, M. Morbidelli, Comp. Chem. Eng. 21 (1997) 641.
[12] K. Kaczmarski, D. Antos, J. Chromatogr. A 862 (1999) 1.
[13] D. Antos, W. Piatkowski, K. Kaczmarski, J. Chromatogr. A 874 (2000) 1.
[14] D. Antos, K. Kaczmarski, W. Piątkowski, A. Seidel-Morgenstern, J. Chromatogr. A 1006 (2003) 61.
[15] A. Mersmann, Chemie Ingenieur Technik 72 (2000) 17.
[16] A.E. Nielson, Kinetics of Precipitation, Pergamon Press, Oxford, 1964.
[17] H. Schubert, A. Mersmann, Trans. Inst. Chem. Eng. A 74 (1996) 821.